

# UC Davis

## UC Davis Previously Published Works

### Title

Generating Monoclonal Antibodies against Buprofezin and Developing Immunoassays for Its Residue Detection in Tea Samples

### Permalink

<https://escholarship.org/uc/item/27h3d8f0>

### Journal

Journal of Agricultural and Food Chemistry, 71(41)

### ISSN

0021-8561

### Authors

Xu, Lingyuan

Aty, AM Abd El

Cao, Zhen

et al.

### Publication Date

2023-10-18

### DOI

10.1021/acs.jafc.3c03263

Peer reviewed



Published in final edited form as:

*J Agric Food Chem.* 2023 October 18; 71(41): 14967–14978. doi:10.1021/acs.jafc.3c03263.

## Generating Monoclonal Antibodies against Buprofezin and Developing Immunoassays for Its Residue Detection in Tea Samples

Lingyuan Xu<sup>a</sup>, A.M. Abd El-Aty<sup>b,c,d</sup>, Zhen Cao<sup>a</sup>, Xingmei Lei<sup>a</sup>, Jing Zhao<sup>a</sup>, Jia Li<sup>e</sup>, Song Gao<sup>a</sup>, Yun Zhao<sup>a</sup>, Yongxin She<sup>a</sup>, Fen Jin<sup>a</sup>, Jing Wang<sup>a</sup>, Maojun Jin<sup>a,\*</sup>, Bruce D. Hammock<sup>f</sup>

<sup>a</sup>Institute of Quality Standard and Testing Technology for Agro-Products, Chinese Academy of Agricultural Sciences, Beijing 100081, China

<sup>b</sup>Department of Pharmacology, Faculty of Veterinary Medicine, Cairo University, Giza 12211, Egypt

<sup>c</sup>State Key Laboratory of Biobased Material and Green Papermaking, Qilu University of Technology, Shandong Academy of Sciences, Jinan, 250353, China

<sup>d</sup>Department of Medical Pharmacology, Medical Faculty, Ataturk University, Erzurum 25240, Turkey

<sup>e</sup>Jinhua Miaozhidizhi Agricultural Technology Co., Ltd., Jinhua 321000, China

<sup>f</sup>Department of Entomology & Nematology and UC Davis Comprehensive Cancer Center, University of California, Davis, CA 95616, USA

### Abstract

The synthesis of a hapten and antigen for the preparation of a monoclonal antibody (mAb) for buprofezin is described. The recognition mechanism of hapten and buprofezin by the monoclonal antibody (mAb-19F2) is described. The effectiveness of the mAb-19F2 immunoassay technique was assessed, and effective detection of buprofezin in tea samples was achieved through the establishment of ic-ELISA and colloidal gold immunochromatography. The mAb-19F2 subtype was IgG<sub>1</sub>, with an IC<sub>50</sub> of 1.8 ng/mL and a linear range (IC<sub>20</sub>-IC<sub>80</sub>) of 0.6 µg/L-5.4 µg/L, and had a cross-reaction rate of less than 0.18% with 29 other pesticides (neonicotinoids and insect growth regulators). The study identified  $\pi$ - $\pi$  stacking interactions between hapten and TYR-61 at the mAb-19F2 site and alkyl/Pi-alkyl interactions with TRP-105 and ARG-103. The ic-ELISA had an IC<sub>50</sub> of 12.9 ng/mL in green tea and 5.65 ng/mL in black tea, with a recovery rate of 92.4%–101.0% and RSD of 2.1%–4.8%. The gold immunochromatographic assay (GICA) had a

\*Corresponding authors: Maojun Jin, jinmaojun@caas.cn, Tel. : +86-10-8210-6570.

Declaration of competing interest

The authors declare that there are no conflicts of interest.

Animal Experiment Statement

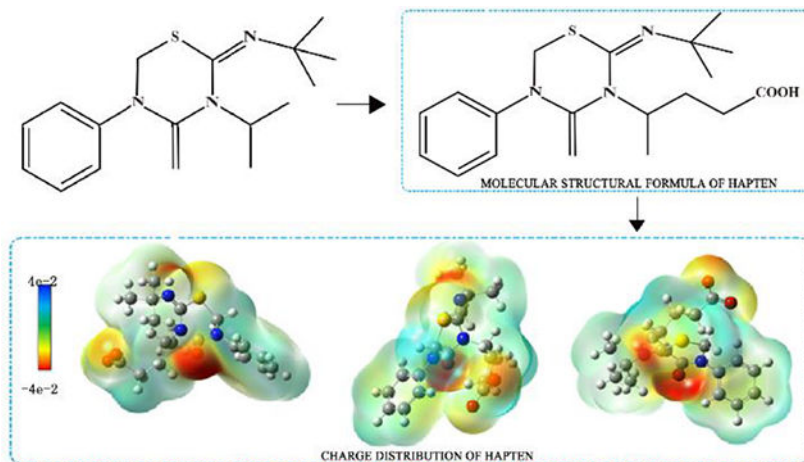
The animal study protocol was approved by the Experimental Animal Welfare and Ethical Committee of the Institute of Quality Standards and Testing Technology for Agro-Products, Chinese Academy of Agricultural Sciences (IQSTAP-2021-05).

The supporting information

Additional experimental details, materials, and methods, including characterization of haptens and complete antigens, and photos of colloidal gold characterization.

detection limit (LOD) of 500 ng/mL, with the complete disappearance of test lines visible to the naked eye. The limit of quantitation (LOQ,  $IC_{20}$ ) was determined to be 16.8 ng/mL. Additionally, the developed GICA showed no cross-reactivity with neonicotinoid pesticides. The recovery rate of tea spiked recovered samples was 83.6%–92.2%, with an RSD of 5.3%–12.6%, and the results were consistent with the LC/MS method. This study is important for the real-time detection of buprofezin residues to ensure food safety and human health.

## Graphical Abstract



## Keywords

Buprofezin; Hapten; Molecular docking; Colloidal gold; Immunoassay

## 1. Introduction

Nihon Nohyaku Co., Ltd. (Tokyo, Japan) developed buprofezin for registration in 1983,<sup>1</sup> which is an insect growth regulator (IGR).<sup>1</sup> Its chemical formula is  $C_{16}H_{23}N_3SO$ , and its relative molecular weight is 305.4. The substance is a white crystal with a melting point of  $104.5\text{ }^{\circ}\text{C}$ – $105.5\text{ }^{\circ}\text{C}$  and a relative density of 1.18 ( $25\text{ }^{\circ}\text{C}$ ), and it is stable under conditions of acid, alkali, light, and heat. The effect of buprofezin on the development and reproduction of white-backed planthopper is sublethal.<sup>2</sup> Buprofezin is classified as an insect growth regulator of the heterocyclic thiazine class. Its mode of action involves inhibiting insect chitosan synthesis and thus disrupting insect metabolism and development.<sup>3</sup> It possesses a potent contact-killing effect that can cause nymphs to molt prematurely or develop wing deformities, leading to eventual death.<sup>4</sup> The toxic effects of thiazide on various pests have been reported, including pests such as *chrysoperla carnea* (stephens) (Neuroptera: Chrysopidae),<sup>5</sup> *chrysoperla rufilabris* (Neuroptera: Chrysopidae),<sup>6</sup> melon aphid<sup>7</sup> and brown planthopper.<sup>8</sup> The substance is particularly effective in controlling planthopper, leafhopper, whitefly, and shellfish pests<sup>9</sup>.

Buprofezin has found widespread use in pest control for various crops, such as tea, rice, fruit trees, and vegetables, due to its unique mechanism of action, high selectivity, and biosafety

at recommended doses. It is often incorporated into pest control rotation schemes and widely used worldwide for integrated pest management (IPM). The prohibition of highly toxic pesticides and the increasing resistance of pests to conventional pesticides. Buprofezin is used as a pest management tool and has great value in protecting the quality of agricultural products during all planting stages. Buprofezin has a long shelf life, but its use must be carefully managed to prevent the accumulation of residues in the environment. Buprofezin is currently registered and used in over 60 countries, and there is relatively little research on the toxic effects of residual buprofezin. There have been reports of its toxicity to aquatic organisms,<sup>10</sup> but there is a lack of extensive toxicity research on aquatic organisms. Chronic and subchronic exposure to buprofezin residues can affect the liver and thyroid. Current research has found that buprofezin can cause teratogenesis in the embryos and larvae of African catfish,<sup>11</sup> while zebrafish produces synergistic embryotoxicity.<sup>12</sup> Some countries have banned its use due to its toxicity to aquatic organisms and humans.<sup>10</sup> Therefore, it is necessary to detect the residual level of buprofezin.

The instrument detection methods for IGRs insecticides mainly include gas chromatography (GC) (GB/T 5009.184–2003; SN/T 1594–2019), GC with ion trap mass spectrometry (GC/ITMS),<sup>1</sup> high-performance liquid chromatography (HPLC) (Ding et al., 2019),<sup>13</sup> gas chromatography-tandem mass spectrometry (GC–MS/MS),<sup>14</sup> and liquid chromatography-tandem mass spectrometry (HPLC–MS/MS).<sup>15</sup> Confirmatory analysis methods provide better sensitivity, precision, and accuracy but are expensive and have slow analysis speeds, as sample preparation is complex. These methods cannot meet the needs of rapid on-site detection. Rapid analysis technology, on the other hand, provides quick on-site analysis and can timely and effectively identify risks through rapid screening. This technology is characterized by simple operation, miniaturization, convenience, and low cost.<sup>16</sup>

As public health awareness and living standards improve, the health risks posed by pesticide residues in agricultural products and food are becoming a growing concern. In recent years, tea has been gaining recognition as a healthy beverage with unique health benefits.<sup>17</sup> Consumers are paying more attention to the quality of tea and the issue of pesticide residues. To ensure consumer safety and regulate international trade, many countries and international organizations have established maximum residue limits (MRLs) for neonicotinoid pesticide residues in agricultural products. The European Commission and some government agencies have also set MRLs for several neonicotinoids in tea. The MRLs for neonicotinoids in European Union (EU) tea range from 0.05 to 20 mg/kg,<sup>18</sup> and the MRL range is 10 to 50 mg/kg in Japan.<sup>19</sup> In China, the Ministry of Agriculture has stipulated an MRL of 10 mg/kg for buprofezin in tea beverages according to GB 2763–2021. Excessive pesticide residues can seriously affect the trade, circulation, and development of tea-related industries, making monitoring of pesticide residues in tea essential for accurately assessing human exposure to pesticides through beverages.

As one of the mainstream research avenues for rapid detection technology, immunoassays possess good characteristics, making them a crucial component in guaranteeing the quality and safety of agricultural products. Thus, the attributes of immunoassays of high sensitivity and resistance to matrix effects make them particularly useful for monitoring residues in tea.

Such applications range from field tests insuring the proper use of the pesticide through high throughput analysis guaranteeing low residues in products shipped internationally.

Consequently, we synthesized the hapten and complete antigen of buprofezin, generated multiple monoclonal antibodies, and selected one monoclonal antibody (mAb-19F2) to investigate its recognition mechanism for the first time, thereby bridging a current research gap. This work led to the development of successful immunoassay methods for the real-time detection of buprofezin residues. This understanding of binding dynamics assisted in the optimization of mAb-19F2 in a practical field and high-throughput assay, and it will undoubtedly contribute to ensuring the quantity, quality and safety of agricultural products and ultimately benefit public health. More generally, this understanding of hapten-antibody interactions will inform future hapten design for other immunoassays.

## 2. Reagents and materials

The following reagents and consumables were acquired from Shanghai Anneji Chemical (Shanghai, China) for the synthesis of hapten antigen: 5-methyl-2-pyrrolidone ( $C_5H_9NO$ ), sulfoxide chloride ( $SOCl_2$ ), *tert*-butyl isosulfate ( $C_5H_9NS$ ), silica gel column (200~300 mesh), tetrahydrofuran ( $C_4H_8O$ ), ethyl acetate ( $C_4H_8O_2$ ), *N*-methylformanilide ( $C_8H_9NO$ ), carbon tetrachloride ( $CCl_4$ ), sulfonyl chloride ( $SO_2Cl_2$ ), tetrabutylammonium bromide ( $C_{16}H_{36}BrN$ ), 1,4-dioxane ( $C_4H_8O_2$ ), and triethylamine ( $C_6H_{15}N$ ). Meanwhile, hydrochloric acid (HCl), methanol ( $CH_3OH$ ), sodium bicarbonate ( $NaHCO_3$ ), dichloromethane ( $CH_2Cl_2$ ), petroleum ether, tetrahydrofuran ( $C_4H_8O$ ), sodium hydroxide (NaOH), formic acid (HCOOH), Azodiisobutyronitrile (AIBN), and nitrogen ( $N_2$ ) were obtained from Sinopharm Chemical Reagent Co., Ltd. (Shanghai, China), Shanghai Aladdin Biochemical Technology Co., Ltd. (Shanghai, China), and Beijing Shunanqite Gas Co., Ltd. (Beijing, China), respectively. Reagents and consumables used for complete antigen synthesis, monoclonal ligation tumor preparation, and indirect enzyme-linked immunosorbent assay were consistent with previous research reports.<sup>20,21</sup> Sartorius (Gottingen, Germany) supplied the nitrocellulose film (NC film) with a CN120 model, which was used for making the test strips. Jieyi Biotechnology Co., Ltd. (Shanghai, China) provided the sample pad, polyvinyl chloride (PVC) board, and absorbent pad. Chloroauric acid ( $HAuCl_4 \cdot 3H_2O$ ) and trisodium citrate were procured from Sigma–Aldrich (St. Louis, USA), while *N*-propylethylenediamine (PSA), octadecyltrimethoxysilane ( $C_{18}$ ), acetonitrile (chromatographic grade), and methanol were obtained from Tianjin Bona Ejer Technology Co., Ltd. (Tianjin, China).

### 2.1 Design and synthesis of haptens

**2.1.1 Hapten Design and Molecular Characterization**—To maximize the exposure of the antigen determinant of the target activator to the immune system, the hapten designed in this study features a short spacer arm (one spacer arm) that positions it away from the carrier protein. The carboxyl ( $-COOH$ ) group was chosen as the active group in the hapten terminal design, in part because the coupling reaction between carboxyl and carrier protein can be conducted at room temperature to not denature or precipitate the carrier protein (25 °C).

This study utilized ACD/Percepta to predict and examine the physicochemical characteristics of the formulated buprofezin Hapten. The findings are presented in Figures S4–S5. The predictions reveal that the Log P value for the designed hapten is 3.06, whereas the Log P value estimated by the molecular structure formula of buprofezin is 3.56. This suggests that the hydrophilicity of the buprofezin hapten surpasses that of the original buprofezin structure. Furthermore,  $V_x$  notably increased from 2.45 to 2.81.

After constructing the molecular structural formula with Chem 3D, the molecular surface electrostatic potential was plotted using Gaussian 09 and Gaussian View programs. Structural optimization was carried out first using the apfd/6–31 g (d) theoretical level, followed by calculation of the optimized structure using the apfd/6–311 + g (2d, p) theoretical level for single point energy. Based on the calculated FCHK file, the molecular surface electrostatic potential was further plotted using the GaussView program, and the resulting surface electrostatic potential of haptens is displayed in Figure 1(A). The hapten designed in this study retains many of the physical and chemical properties of the target compound, including molecular weight, spatial conformation, and electronic configuration, without significant changes.

## 2.1.2 Synthesis of the hapten

**2.1.2.1 Synthesis of Thiourea Fragments:** A-1: In a 100 mL round bottom flask, an aqueous solution of 5-methyl-2-pyrrolidone (9.9 g, 100 mmol, 1.0 equiv) and 50 mL of 6 M hydrochloric acid was added at room temperature (25 °C). The mixture was refluxed at 100 °C for 8 h with a condensing tube. The completion of the reaction was supported by monitoring on silica gel TLC. The resulting product was posttreated by cooling to room temperature (25 °C), concentrating under vacuum, dissolving with methanol, and concentrating under vacuum 3 times. The resulting product was pure enough for use in the next reaction.

A-2: The crude product from A-1 was dissolved in dry methanol (100 mL) at room temperature, and dichlorosulfoxide (14.5 mL, 200 mmol, 2.0 equiv) was added dropwise under nitrogen protection. The mixture was then refluxed at 80 °C for 6 h. TLC monitoring confirmed completion of the reaction, followed by cooling to room temperature and vacuum concentration. The concentrated solution was dissolved in methanol, and this process was repeated three times, yielding a pure product suitable for the subsequent reaction.

A-3: The crude product from A-2 was dissolved in 100 mL of dried dichloromethane at room temperature (25 °C).  $\text{NaHCO}_3$  (16.8 g, 200 mmol, 2.0 equiv) was added under nitrogen protection and stirred evenly, followed by the slow addition of tertiary butyl isosulfate (15.2 mL, 120 mmol, 1.2 equiv) while stirring. The reaction was continued under nitrogen protection for 10 h at room temperature, and TLC monitoring confirmed completion of the reaction. The resulting mixture was filtered to remove solid  $\text{NaHCO}_3$ , and the filtrate was concentrated under reduced pressure and purified using a silica gel column with a mobile phase of petroleum ether/ethyl acetate ranging from 20:1 to 5:1. This yielded 16.8 g of pure A-3 with a three-step yield of 68.3% from A-1 to A-3.

A-4: To a solution of apparently pure A-3 (16.8 g, 68.3 mmol, 1.0 equiv) in 70 mL of tetrahydrofuran at room temperature, slowly add a solution of NaOH (5.46 g, 136.5 mmol, 2.0 equiv) in 70 mL of water under stirring, and slowly drip the obtained NaOH solution into the solution of A-3. After 5 h of reaction at room temperature (25 °C), TLC monitoring indicated completion of the reaction (TLC conditions). The reaction mixture was treated by removing tetrahydrofuran under reduced pressure, adjusting the pH to 3–5 with 2 N hydrochloric acid, and extracting the aqueous phase with ethyl acetate three times (100 mL × 3). The combined organic phases were dried, filtered, and concentrated under reduced pressure to obtain the crude product. The crude product was purified by silica gel column chromatography using petroleum ether/ethyl acetate/formic acid (2/1/0.05 to 1/1/0.05) as the mobile phase. Pure A-4 (12.7 g) was obtained in 80.1% yield.

**2.1.2.2 Synthesis of Acyl Chloride Fragments:** B-1: N-Methylformaniline (2.46 mL, 20 mmol, 1.0 equiv), AIBN (263 mg, 1.6 mmol, 0.08 equiv), and carbon tetrachloride (20 mL) were added to a reaction flask at room temperature under nitrogen protection. The mixture was heated to 70 °C, and sulfonyl chloride (4.86 mL, 60 mmol, 3.0 equiv) was added slowly. The reaction was continued at 90 °C for 3 h, and TLC monitoring confirmed completion of the reaction. The crude product was obtained and directly used for the next reaction after solvent removal under reduced pressure.

**2.1.2.3 Synthesis of target hapten:** The synthesis pathway of the target hapten is shown in Figure 1 (B). At room temperature (25 °C), A-4 (232 mg, 1.0 mmol, 1.0 equiv), tetrabutylammonium bromide (64 mg, 0.2 mmol, 0.2 equiv), and 8 mL of 1,4-dioxane were added to a reaction tube. The mixture was thoroughly mixed and then slowly treated with 1.2 mL (3.0 equiv) of 10% aqueous sodium hydroxide solution. Then, a solution of B-1 (305 mg, 1.5 mmol, 1.5 equiv) in 2 mL of 1,4-dioxane was slowly added to the reaction system. The mixture was stirred for 8 h at room temperature, and the reaction was considered complete according to TLC monitoring. The 1,4-dioxane is removed by decompression and concentration after the reaction. The pH of the solution was adjusted to 3–5 with 2 N HCl, and the aqueous phase was extracted with ethyl acetate (100 mL × 3) three times. The organic phases were combined, dried, filtered, and concentrated under reduced pressure to yield the crude product. The crude product was purified by using a silica gel column with mobile phase conditions of petroleum ether/ethyl acetate/triethylamine (from 2:1:0.05 to 1:1:0.05). The resulting pure product with a yield of 14.3%, 52 g, was obtained.

## 2.2 Preparation of complete antigen

Pesticide haptens are small molecules that exhibit immunoreactivity but lack immunogenicity. To prepare an immunogenic complete antigen, the small molecule hapten of the pesticide needs to be coupled with a large molecule carrier protein. However, the complete antigen cannot be directly used to immunize host animals. It needs to be emulsified with adjuvant to enhance its immunogenicity, and the resulting emulsified complete antigen can be used for immunization. The synthetic route of the complete antigen is illustrated in Figure 1(C).

In this study, BSA and OVA were chosen as the immunogen carrier protein and coating carrier protein, respectively. The active group of the pesticide hapten was carboxyl, and the complete antigen was prepared using the active ester method. Before the synthesis of the complete antigen, theoretical calculations were performed to determine the amounts of hapten, N-hydroxysuccinimide (NHS), and 1-(3-dimethylaminopropyl)-3-ethylcarbodiimide hydrochloride (EDC) to be added. For instance, when the molar ratio of hapten to carrier protein (BSA/OVA) was 50:1, the specific procedure for the preparation of complete antigen was followed. A magnetic rotor was added to a brown glass vial containing hapten (9.63 mg, 0.027 mmol), NHS (6.21 mg, 0.054 mmol), and EDC (10.35 mg, 0.054 mmol), followed by the addition of 1 mL of anhydrous N,N-dimethylformamide (DMF) to dissolve the mixture. The solution was then refrigerated at 4 °C for the activation reaction and magnetically stirred for 10 h. The activation reaction product was obtained, which was used for the subsequent coupling reaction. A 10 mg/mL OVA solution and a 20 mg/mL BSA solution were prepared with 0.01 mol/L phosphate buffer solution (PBS, pH=7.4). The coupling reaction was conducted at room temperature on a magnetic stirrer. The supernatant obtained from the activation reaction was added dropwise to 429  $\mu$ L of 10 mg/mL OVA solution and 571  $\mu$ L of 20 mg/mL BSA solution. The reaction solution was stirred at 25 °C for 4 h, and dialysis with 0.01 mol/L PBS (pH=7.4) solution was performed six times. After dialysis, the complete antigen was subpacked and then frozen in liquid nitrogen. The freeze-dried complete antigen protein powder was stored in a refrigerator at -20 °C for further use.

### 2.3 Preparation of monoclonal antibody

This study involved the use of six female BALB/c mice, aged 7 weeks, following the same monoclonal preparation as previously reported<sup>20</sup>. The buffer solution for the ic-ELISA method utilized in this study was prepared and operated according to previous studies<sup>20,21</sup>. The ic-ELISA method was employed to detect the antiserum titer of the six mice. Table S1 displays the determination results of the serum titer and inhibition rate of anti-buprofezin in the mice selected for fusion. The procedures for ascites antibody preparation and purification were conducted in accordance with previous reports<sup>20,21</sup>. The purified ascites antibodies were freeze-dried and stored in a refrigerator at -20°C. To prepare for subsequent experiments, a 1 mg/mL antibody solution containing 50% glycerol was made.

### 2.4 Establishment of ic-ELISA method

To ensure the stability and low detection limit of the ic-ELISA method established in this study, various factors affecting its stability were investigated. The factors include the concentration of NaCl in the sample solution, pH value, organic solvents (methanol and acetonitrile content), and reaction time of the second antibody (IgG-HPR). To optimize the conditions of the ic-ELISA method, the antigen and antibody were diluted to an optimal combination, and gradient diluted standards of different concentrations of buprofezin were prepared. Under the constant dilution ratio of antigen and antibody, the OD<sub>450 nm</sub> value was calculated under different reaction conditions using the controlled variable method. Each optimization condition was set up with an experimental group and a blank group, and all experiments were performed in triplicate. The ratio (B/B<sub>0</sub>) of the OD<sub>450 nm</sub> value of the inhibition well to the control well was plotted as a standard curve for each optimization condition. The value of B/B<sub>0</sub> was calculated based on the measured OD<sub>450 nm</sub> value, and



the standard curve was fitted according to the calculated results. The abscissa represents the concentration of the buprofezin standard, and the ordinate represents the measured value of  $B/B_0$ . The main aim was to identify and optimize the reaction conditions that primarily affect the ic-ELISA method.

#### **2.4.1 Determination of the optimum concentration of antigen and antibody—**

Dilute the 1 mg/mL coated original solution and 1 mg/mL antibody solution using gradient dilution to the appropriate concentration required for the experiment. The ic-ELISA method was employed to determine the most suitable combination of antibody and antigen dilution concentrations for detecting the inhibition concentration of buprofezin pesticide at 100 ng/mL. The results of this optimization procedure are presented in Table S2, which indicated that the most suitable dilution concentration combination for the reaction was an antigen dilution of  $4 \times 10^3$  times and an antibody dilution of  $4 \times 10^3$  times.

#### **2.4.2 Optimization of reaction conditions—**

To determine the optimal conditions for the ic-ELISA method, various experiments were conducted. The pesticide standard was first diluted using sample dilute buffer solutions with pH values ranging from 5.5 to 9.5, and the ic-ELISA method was used for determination. Similarly, the pesticide standard was diluted with sample dilutions containing NaCl concentrations ranging from 0.05 mol/mL to 0.2 mol/mL and with sample diluents containing different organic reagents (methanol and acetonitrile). The ic-ELISA method was used to determine the results in all experiments. To optimize the reaction time after the addition of the second antibody (IgG-HPR), different reaction times were set (15 min, 30 min, 45 min, and 60 min), and the results were measured using the ic-ELISA method.

#### **2.4.3 Processing of tea samples—**

The tea sample utilized in this study was acquired from a local supermarket in Beijing, and no residue of buprofezin pesticide was detected in the sample through liquid chromatography–mass spectrometry (LC–MS). Figure S8 and Figure S9 display the determination results. A standard solution of buprofezin pesticide was prepared using acetonitrile at concentrations of 1 mg/mL, 100  $\mu$ g/mL, and 1  $\mu$ g/mL. The pretreatment steps of tea samples for ic-ELISA method determination and LC–MS determination were conducted in accordance with GB-23200.121–2021. The specific operational steps are thoroughly explained in the supplementary materials. The supernatant utilized for ic-ELISA determination was dried with nitrogen, and its recovery was determined by redissolving it with PBSTG containing 5% acetonitrile, as needed.

To determine a tea sample with a colloidal gold strip, a test tube was used to accurately weigh 1 g of tea sample (black and green tea, with an accuracy of 0.01 g). Subsequently, 50 mL of boiling water was added to the tube, and the mixture was allowed to soak for 30 min. The tea infusion was then extracted, and its pH was measured. The pH of the tea infusion was adjusted to 6–7, and 100  $\mu$ L was taken for the determination of test strips. The added recovery concentrations used in this study were 2.5 mg/kg (1/4 MRL), 5 mg/kg (1/2 MRL), and 10 mg/kg (MRL), given that the solubility of buprofezin in water was 9 mg/L (20 °C).

## 2.5 Development of immunochromatographic test strip

**2.5.1 Preparation of colloidal gold**—To set up the experiment, an iron stand and a condensation reflux device were arranged, and the switches for digital heating and stirring electric heating jackets were turned on. Next, ultrapure water was added to a three-hole round bottom flask in varying amounts (245 mL, 240 mL, and 230 mL) and placed in a magnetic stirring rotor. The heating temperature was set to 100 °C, and the rotational speed was set to 300 rpm/min. Three different ratios of colloidal gold were prepared using 1% sodium citrate solution and 1% chlorogold acid, with ratios of 1:1, 2:1, and 4:1. Once the water in the flask boiled and uniform bubbles were generated, 1% sodium citrate solution (5 mL, 10 mL, and 20 mL) was quickly added, followed by 5 mL of 1% chloroauric acid. As the solution in the flask turned from colorless to black and then to purple, the heating source was turned off when the solution turned wine red and remained that color. The magnetic stirring reaction was continued for 10 min after the heat source was turned off. Upon completion of the reaction, the magnetic stirring was turned off, and the condensation reflux device was removed. The colloidal gold solution was then poured into a brown glass bottle, cooled, and stored in a refrigerator at 4 °C. Finally, transmission electron microscopy (TEM) was used to analyze the particle size and morphology of the three types of colloidal gold synthesized.

### 2.5.2 Condition optimization

**2.5.2.1 Optimization of Gold Labeled Antibodies:** The pH of the gold-labeled antibody was optimized. Then, 1 mL of colloidal gold solution with a particle size of 40 nm, as determined by transmission electron microscopy (TEM), was added sequentially to each centrifuge tube. Starting from left to right, 0.1 M K<sub>2</sub>CO<sub>3</sub> was added (2 μL to 9 μL). After vortex mixing, 10 μL of 1 mg/mL mAb-19F2 was added to each centrifuge tube. The mixture was allowed to react at room temperature (25 °C) for 10 min on a blender, and the color change of the colloidal gold solution was observed. The optimal pH was selected as the amount of 0.1 mol/L K<sub>2</sub>CO<sub>3</sub> that did not significantly change the color of the colloidal gold after the reaction was completed. Subsequent optimization was then carried out.

Sequentially add 1 mL of 40 nm colloidal gold solution to each centrifuge tube. Next, the optimized amount of 0.1 mol/L K<sub>2</sub>CO<sub>3</sub> was added into each centrifuge tube from left to right. After vortex mixing, mAb-19F2 was added at a concentration of 1 mg/mL in gradients of 5 μL to 35 μL. The reaction mixture was blended at room temperature for 10 min and then closed by adding 30 μL of 10% BSA solution for 20 min. Finally, the mixture was centrifuged at 10000 rpm for 10 min.

**2.5.2.2 Solution optimization for resolution of gold-labeled probe:** To optimize the surface active agent, Triton 100 (0.05%), Tween 20 (0.05%), and PEG 20000 (0.05%) were selected. A single variable was controlled while the other formulation solutions remained constant, including PB (0.02 M) solution, trehalose (2.5%), and BSA (0.5%). Three complex solutions were prepared using these ingredients to determine the optimal surface active agent. To evaluate the color rendering properties of the test strips, four complex solution formulations were prepared. These included PB solution (0.02 M) + BSA (0.5%) + PEG-2000 + sucrose (2.5% (#1) and 5% (#2)) and PB solution (0.02 M) + BSA (0.5%)

+ PEG-2000 + trehalose (2.5% (#3) and 5% (#4)). The optimized surfactant and selected complex solution formula were used to determine the color development performance of the test strip. Five gradients were set for the complex solution, ranging from 100  $\mu\text{L}$  to 500  $\mu\text{L}$  each.

**2.5.2.3 Optimizing the dilution concentration of coated and goat anti-mouse IgG:** The C line was coated with goat anti-mouse IgG, and the T line was coated with buprofezin antigen (hapten-OVA). The detection performance and color rendering effect of the test strip were influenced by the dilution ratio of both. Hence, an optimal combination was determined to ensure that the test strip met the standards for detecting buprofezin residues.

**2.5.2.4 Optimization of Sample Dilution Buffer Solution:** PBS (0.1 M, 0.05 M) solution and PB (0.2 M, 0.1 M) solution were prepared, the color development effect of the test strip was measured, and a buffer with a better color development effect was selected to dilute the tea sample.

**2.5.3 Assembly and evaluation of test strips—**Herein, the required gold label pad, NC film, absorbent paper, and sample pad were overlapped by 1–2 mm using the main assembly method. The gold label pad, sample pad, and partially assembled absorbent paper were then assembled on the bottom plate. The resulting test strip was cut into a fixed size (4 mm  $\times$  60 mm) using an automatic test strip cutting machine and was subsequently used for experiments. This study evaluated the detection limit, tolerance, specificity, and stability of GICA.

### 3. Results and discussion

#### 3.1 Identification of hapten

The hapten synthesis pathway involved three main stages: thiourea segment synthesis, acyl chloride segment synthesis, and final hapten synthesis. The synthesized compound was analyzed using high-resolution mass spectrometry (HRMS), nuclear magnetic resonance hydrogen spectroscopy ( $^1\text{H}$  NMR), and carbon spectroscopy ( $^{13}\text{C}$  NMR). The characterization results confirmed that the synthesized compound had the expected hapten design, as depicted in Figure S1–S3. The  $^1\text{H}$  NMR and  $^{13}\text{C}$  NMR characterization data for the hapten structure are as follows:  $^1\text{H}$ NMR (400 M,  $\text{CDCl}_3$ ):  $\delta$  1.33 (s, 9, tBu), 1.49 (d, 3,  $J=8.0$  Hz, CH3), 2.02–2.11 (m, 1, H4–1), 2.40 (t, 2,  $J=8.0$  Hz, H3), 2.55–2.48 (m, 1, H4–1), 4.61–4.55 (m, 1, H5), 4.76 (d, 1,  $J=12.0$  Hz, H2–1), 4.82 (d, 1,  $J=12.0$  Hz, H2–1), 7.22–7.40 (m, 5, Ph).

$^{13}\text{C}$  NMR (101 MHz, DMSO)  $\delta$  174.33, 154.49, 142.61, 141.42, 128.79, 125.81, 124.84, 53.84, 53.80, 47.11, 45.46, 40.12, 39.91, 39.70, 39.50, 39.29, 39.08, 38.87, 31.63, 29.29, 28.96, 18.36, 9.99.

The HRMS analysis indicated that the expected molecular structure of  $\text{C}_9\text{H}_{14}\text{ClN}_5\text{O}_2$  was achieved, with a  $[\text{M}+\text{H}^+]$  value of 363.16 and a found value of 364.1712.

### 3.2 Characterization of complete antigen

The complete antigens (coated antigen and immunogen), BSA and OVA standards that were synthesized in this study were analyzed using matrix-assisted laser desorption/ionization time of flight mass spectrometry (MALDI-TOF-MS). The ion peak mass charge ratios of BSA and OVA standards were 67334.280 and 44152.499, respectively. The coupling ratio between hapten and carrier protein was calculated using a formula, and the results are presented in Table 1. The MALDI-TOF-MS measurement spectrum is depicted in Figure S6–S7. The molecular weight of the hapten was determined to be 363.16. The coupling ratio between hapten and carrier protein was calculated using a previously reported formula, and the calculation result was rounded to the nearest integer. The coupling ratio of the coated antigen was 1:4, while the coupling ratio of the immunogen was 1:16.

### 3.3 Evaluation of mAb-19F2 performance

**3.3.1 Sensitivity**—A gradient of half-dilutions of the original coated PBSTG solution can be prepared by diluting it to a concentration of 1 mg/mL. Similarly, a gradient of PBSTG solutions can be prepared by diluting the antibody solution to a concentration of 1 mg/mL. The optimal dilution concentration combination of antigen and antibody (mAb-19F2) was determined using the ic-ELISA method, where the inhibitory concentration of buprofezin pesticide was 100 ng/mL. As shown in Table S2, the antigen was diluted  $4 \times 10^3$  times, and the antibody was diluted  $4 \times 10^3$  times. For the specific detection of buprofezin antibodies (mAb-19F2), a positive hybridoma cell line was selected in this study. The  $IC_{50}$  value of the selected cell line was 1.81  $\mu\text{g/L}$ , and the measurement range of the mAb-19F2 standard curve ( $IC_{20}$  -  $IC_{80}$ ) was 0.61  $\mu\text{g/L}$  - 5.40  $\mu\text{g/L}$ . The measurement results are shown in Figure 3 (A).

**3.3.2 Specificity**—The ic-ELISA method was employed for specific detection of antibodies under the optimal working concentration of the coating agent and mAb-19F2 antibody. A competitive concentration of 1000 ng/mL neonicotinoids was set. Table 2 shows the results of the cross-reaction of mAb-19F2 antibody against buprofezin and 29 pesticides (neonicotinoids and IGRS). mAb-19F2 demonstrated specificity for buprofezin, and the cross-reaction rates with the other pesticides were less than <0.18%.

**3.3.3 Determination of antibody type**—The antibody type of mAb-19F2 was determined using the mouse antibody type determination kit following the manufacturer's instructions. Three repeated experiments were performed, and the results are presented in the Table below. It was confirmed that mAb-19F2 is an IgG<sub>1</sub> antibody.

**3.3.4 Antibody affinity**—The evaluation of antibody performance relies on several important parameters, and among them, the affinity of the antibody is crucial. Thus, in this study, the relative affinity value of mAb-19F2 was determined using amine thiocyanate ( $\text{NH}_4\text{SCN}$ ). The experimental process followed that of ic-ELISA. After measuring the  $OD_{450 \text{ nm}}$  of mAb-19F2 dissociated with amine thiocyanate and coated antigen and fitting the standard curve, the affinity of mAb-19F2 ( $IC_{50}$  of the standard curve) was determined to be 1.04 mol/L. The measurement results are shown in Figure 3 (B).

### 3.3.5 Recognition mechanism of mAb-19F2

**3.3.5.1 Homogeneous modeling:** In recent years, recognizing intermolecular interactions and predicting the structure of receptor–ligand complexes through computer-aided drug design has emerged as a significant and well-established approach. This method involves simulating the geometric structure and intermolecular forces of molecules, supported by disciplines such as chemometrics, to facilitate direct drug design. Macromolecular docking, as a crucial aspect of this approach, enables the in-depth study of interactions between ligands (drug molecules) and their receptors (known target proteins or active sites). It allows for the prediction of binding modes and affinity, as well as the identification and optimization of drug lead molecules. Consequently, this technique enables drug design based on structural considerations. The Swiss Model server was utilized to construct the three-dimensional spatial structure of the mAb-19F2 proteins used for docking, with the template protein selected from a protein structure with PDB IDs of 1 ngp. The H-chain homology for mAb-19F2 was 32.32%, and the L-chain homology was 58.46%.

**3.3.5.2 Molecular docking results:** Based on molecular docking with mAb-19F2, the binding complex of buprofezin hapten was obtained, which binds between the heavy (H) and light (L) chains of the target protein. The active pocket is surrounded by the ring structure of the antibody complementarity-determining region (CDRH1–3 and CDRL1–3) (Figure 2(A)). From the interaction diagram (Figure 2(B)), it is evident that the buprofezin hapten mainly interacts with tyrosine (TYR-61) at the mAb-19F2 site in a  $\pi$  -  $\pi$  stacking manner and with tryptophan (TRP-105) and arginine (ARG-103) in a  $\pi$  - alkyl manner. In this complex, a binding affinity score of  $-6.1$  kcal/mol was given for hapten and mAb-19F2.

The sensitivity of small molecule immunoassays is generally improved by handling heterology, coupling heterology and hapten heterology between the immunizing and reporting hapten. The higher the affinity the antibody has for the coating antigen, the more sensitive the immunoassay until that affinity approaches that of the analyte. At this point, the sensitivity of the assay drops dramatically. Usually, this is optimized by using a different coupling chemistry, different handle or spacer and a different hapten. This is often a difficult balance to achieve and illustrates the fundamental disadvantage of a heterologous vs homologous label. However, as the target analyte becomes larger and the attachment side of the hapten to the carrier protein becomes more remote from the antibody recognition site, hapten heterology becomes increasingly less important. In the case of this immunoassay, it has little if any importance.<sup>22</sup>

## 3.4 Optimization results of the Ic-ELISA method

**3.4.1 pH optimization—**The  $IC_{50}$  value of mAb-19F2 was found to be the smallest at pH 5.5, while it was the highest at pH 6.5, indicating that the sensitivity of the antibody was the poorest at this pH, with the  $IC_{80}$  value being the lowest. Furthermore, as the pH of the solution became more alkaline (pH=7.5–9.5), the  $IC_{50}$  value gradually increased, suggesting that the sensitivity of the mAb-19F2 antibody decreased gradually. Notably, mAb-19F2 exhibited higher sensitivity under acidic conditions. These findings indicate that the optimal pH for mAb-19F2 was 5.5. The measurement results are shown in Figure 3 (D).

**3.4.2 Optimization results of NaCl concentration**—At a concentration of 0.05 mol/mL NaCl, mAb-19F2 exhibited the lowest IC<sub>50</sub> value, indicating high sensitivity. However, as the concentration of NaCl gradually increased, both IC<sub>50</sub> and IC<sub>80</sub> values also increased, suggesting a decrease in antibody sensitivity. These results suggest that the optimal concentration of NaCl for mAb-19F2 was 0.05 mol/mL, as depicted in Figure 3 (C) for the optimized determination result. Overall, these findings highlight the influence of NaCl concentration on the sensitivity of mAb-19F2.

**3.4.3 Optimization results of the organic reagent content**—As the concentration of acetonitrile gradually increases, the IC<sub>50</sub> value of mAb-19F2 decreases, indicating that a lower acetonitrile content improves the sensitivity of mAb-19F2 up to a concentration of 12.2 ng/mL. On the other hand, when the concentration of methanol gradually increases, the IC<sub>50</sub> value of mAb-19F2 also increases, suggesting that a higher methanol content reduces the sensitivity of mAb-19F2. The optimal acetonitrile content for mAb-19F2 was determined to be 5%, while the optimal methanol content was 5%, as methanol has a negative impact on mAb-19F2 sensitivity. These results indicate that when using the ic-ELISA method for sample pretreatment, acetonitrile should be used to ensure optimal sensitivity of mAb-19F2. The measurement results are shown in Figure 3 (F) and 3 (G).

**3.4.4 Optimization results of reaction time**—With increasing reaction time of the second antibody (IgG-HPR), the IC<sub>50</sub> value of mAb-19F2 gradually decreases, suggesting that longer reaction times lead to increased sensitivity of mAb-19F2. The optimal reaction time for mAb-19F2 was determined to be 30 min, with an IC<sub>50</sub> value of 1.7 ng/mL. The measurement results are shown in Figure 3 (E).

**3.4.5 Optimizing the ic-ELISA method**—After optimizing the pH of the sample diluent to 5.5, the concentration of NaCl to 0.05 mol/mL, and the reaction time of the second antibody to 30 min as previously determined, a standard curve was established for mAb-19F2 using this optimized sample dilute solution. The IC<sub>50</sub> value of the optimized mAb-19F2 antibody was found to be 1.81 µg/L. The standard curve, which includes the IC<sub>20</sub> to IC<sub>80</sub> range, for the mAb-19F2 antibody had a working range of 0.6 µg/L - 5.4 µg/L. The measurement results are shown in Figure 3 (H).

**3.4.6 Determination of tea samples**—The tea samples used in this study were obtained from a local supermarket in Beijing, and no traces of buprofezin pesticide residues were detected in either black or green tea samples using LC-MS analysis. Using the established ic-ELISA method with mAb-19F2, a standard curve was established for tea (including green tea and black tea) matrices. The fitted curve of the measurement results is shown in Figure 4. The linear range for the green tea matrix was determined to be 0.4 ng/mL to 18.1 ng/mL, with an IC<sub>50</sub> value of 2.4 ng/mL. Similarly, the linear range for the black tea matrix was found to be 0.6 ng/mL to 14.1 ng/mL, with an IC<sub>50</sub> value of 2.5 ng/mL.

### 3.5 Test Strip Development Experiment Results

**3.5.1 Characterization of Colloidal Gold**—In this study, three types of colloidal gold were synthesized using different ratios of 1% sodium citrate solution to 1% chloroauric

acid, specifically at ratios of 1:1, 2:1, and 4:1. The transmission electron microscopy (TEM) characterization results of the synthesized colloidal gold are presented in Figures S10–S13. Among them, the colloidal gold synthesized at a ratio of 1:1 exhibited relatively poor particle size uniformity compared to that synthesized at a ratio of 4:1. This could be due to incomplete reactions resulting from the increased amount of sodium citrate, leading to larger differences in particle size. The particle size of colloidal gold synthesized at a ratio of 1:1 was 40 nm, while that synthesized at a ratio of 2:1 had a diameter of 20 nm. Therefore, a 1:1 ratio of colloidal gold was chosen to achieve better control over reaction conditions such as liquid addition speed, reaction time, and temperature. The resulting colloidal gold particles exhibited the desired size and morphology and were suitable for subsequent experiments.

### 3.5.2 Results of condition optimization

**3.5.2.1 Gold Label Antibody Optimization Results:** The optimal pH for the gold-labeled mAb-19F2 probe was determined based on the results shown in Figure 5(A). The addition of 0.1 M  $K_2CO_3$  (2–5  $\mu$ L) to the gold-labeled probe of mAb-19F2 resulted in significant color changes. The color remained stable at 6  $\mu$ L, indicating that the most suitable pH for adjusting mAb-19F2 was 7  $\mu$ L for further condition optimization.

The absorbance values of the gold-labeled probe were measured using an ultraviolet spectrophotometer with five gradient addition amounts ranging from 400 nm to 600 nm. The measurement results are presented in Figure 5(B). The absorbance value of the mAb-19F2 antibody showed only minor changes as the amount of mAb-19F2 antibody added increased. Based on these findings, this study opted to add 30  $\mu$ L of mAb-19F2 antibody to prepare the gold-labeled probe.

**3.5.2.2 Solution Optimization Results of Gold Label Probe Resolution:** The gold-labeled probe was redissolved using three different complex solutions. The concentration of coated (C lines) was set at 2 mg/mL, and the concentration of secondary antibody (T lines) was set at 0.5 mg/mL. The color development effect was measured using scribing, and the results are depicted in Figure 5(C). PEG-20000 (0.05%) was used on the left, Triton-100 (0.05%) in the middle, and Tween-20 (0.05%) on the right. Based on the color development effect observed, PEG-20000 was chosen for the complex solution in this study.

The color rendering performance of the test strip was evaluated using four different complex solution formulations in this study. The results, shown in the following figure from left to right, include PB solution (0.02 M) + BSA (0.5%) + PEG-20000 + trehalose (2.5% (#1) and 5% (#2)); PB solution (0.02 M) + BSA (0.5%) + PEG-20000 + sucrose (2.5% (#3) and 5% (#4)). Based on the color development results, the selected complex solution formulation for this study was PB solution (0.02 M) + BSA (0.5%) + PEG-20000 + sucrose (5%). This formulation demonstrated the desired color rendering performance for the test strip.

Figure 5(D) shows the measurement results of the complex solution amount, with 100  $\mu$ L of L of complex colloidal gold probe solution exhibiting the deepest color development. As the amount of complex solution increased, the color development of the C and T lines gradually decreased. Therefore, for subsequent experiments, this study selected 100  $\mu$ L of redissolved colloidal gold probe solution.

**3.5.2.2 Optimal dilution combination of antigen and antibody:** The results of the test are presented in Table 4. With an increase in the concentration of the T line, the T/C value of the test strip decreases, indicating difficulty in distinguishing between positive and negative samples using this test strip. The T/C value shows minimal changes, indicating that the sensitivity of detection does not significantly change at this concentration. On the other hand, as the concentration of the coated antigen (C-line) increases, the T/C value of the test strip increases. This suggests that negative samples are easier to distinguish with the naked eye, and the T/C value of positive samples also increases, indicating a decrease in the sensitivity of the test strip under this combination. To ensure that the test strip is easily distinguishable and sensitive for negative samples, this study selected a dilution concentration of 0.3 mg/mL for sheep anti-mouse (IgG, T-line) and 2 mg/mL for the complete antigen (C-line) of buprofezin.

**3.5.2.3. Optimization results of sample dilution buffer:** The effect of various buffer solutions on the color development of the test strip was examined, and the results are presented in Figure 5(F). The color development of the test strip was darkest with 0.01 M PB solution compared to the other three buffer solutions coated with antigen (C-line), as determined by the measurement of purified water. The buffer solutions from left to right are 0.1 M PB, 0.2 M PB, 0.05 M PBS, and 0.1 M PBS.

### 3.6 Performance evaluation of colloidal gold test strips

**3.6.1 Limit of detection—**A standard of buprofezin was prepared using a 0.01 M PBS buffer solution and diluted by half according to a gradient. The test strip developed using this standard had a detection limit (LOD) of 500 ng/mL for complete line elimination visible to the naked eye. The results of the measurement are presented in Figure 6(A). A standard curve was generated based on the T/C values obtained from the test strip, with each measurement repeated three times, and the average T/C value was used for fitting. The T/C value was used to determine the test strip results in this study. An invalid test strip was indicated by the absence of color on the C line. A T/C value of 1 indicated a negative sample, while a T/C value of < 1 indicated a positive sample (above the minimum detection limit of the test strip). The IC<sub>50</sub> of the test strip was 231.20 ng/mL, and the measurement range (IC<sub>20</sub>-IC<sub>80</sub>) was 14.70 ng/mL to 959.43 ng/mL. The curve of the fitted colloidal gold test strip is shown in Figure 6 (B).

**3.6.2 Acetonitrile tolerance—**To investigate the tolerance and color rendering effect of the test strip to acetonitrile, a series of 0.01 M PBS solutions containing acetonitrile (ranging from 5% to 40% with a 5% increment) were prepared. This was done to determine the optimal percentage of acetonitrile that can be present in actual tea samples. The measurement results depicted in Figure 6(C) below show the effect of different percentages of acetonitrile on the color development performance of the test strip. The T/C value was observed to be highest when the acetonitrile content was 40%.

**3.6.3 Specificity—**During the testing of antibody performance, it was observed that mAb-19F2 did not cross react with other neonicotinoids. To assess the specificity of the test strip, we evaluated eight other pesticides for cross-reactivity at a standard concentration of



500 ng/mL. Figure 6 (D) depicts the results, which indicated that none of the eight new nicotine pesticides exhibited cross-reactivity with the test strip. The test strip determination results are consistent with the specificity of the ic-ELISA method for the determination of mAb-19F2. This indicates that the buprofezin test strip developed in this study has good specificity, does not cross react with other pesticides and can be effectively used for the determination of buprofezin pesticide residues in agricultural products.

**3.6.4 Storage stability**—The test strips were stored at room temperature (25 °C), a 37 °C incubator, and a 4 °C refrigerator to determine their stability at different temperatures. The change in the detection limit of the test strips was measured once a week for a total of five weeks. Six parallel blank samples were measured each time, and their average values were taken and plotted. The measurement results, which are shown in Figure 6(E), indicate that good storage performance was observed at 4 °C, and a downward trend in the T/C value was observed with increasing storage time at 37 °C and 5 °C.

**3.6.5 Interbatch stability**—Three batches were developed according to the optimized conditions to determine the stability of the developed test strips within the same development period and between different development periods. Six parallel blank samples were measured for each batch. The measurement results are presented in Figure 6(F).

**3.6.6 Determination of tea samples**—In this study, tea samples were obtained from a local supermarket in Beijing and analyzed for the presence of buprofezin pesticide residue using liquid chromatography–mass spectrometry (LC–MS). However, no residue was detected in the samples. Therefore, the recovery rate was evaluated by spiking buprofezin pesticide into the samples. The average recovery rate of buprofezin using LC–MS/MS was found to be between 92.85% and 110.11% with an RSD of 2.7–7.8%. The accuracy of the analysis results was confirmed by determining the recovery rate of buprofezin pesticide in both black tea and green tea matrices using LC–MS/MS. The determination results, shown in Table 5, indicated that the ic-ELISA method using mAb-19F2 had an average recovery rate of 92.40%–100.96%, with an RSD of 2.1%–4.8%. GICA showed a recovery rate between 83.6% and 92.2%, with an RSD ranging from 4.2%–9.9%. The use of the mAb-19F2-based immunoassay method has shown relatively high accuracy in detecting buprofezin residues in agricultural products and food.

### 3.6 Conclusions

This study accomplished several key objectives. First, it successfully designed and synthesized a buprofezin hapten and generated mAb-19F2, which allowed for the exploration of the recognition mechanism of haptens and mAb-19F2. The study revealed that  $\pi$ - $\pi$  stacking interactions between the hapten and TYR-61 at the mAb-19F2 site occur and that alkyl (alkyl/Pi alkyl) interactions with TRP-105 and ARG-103 occur. The development of these biological materials was a critical step toward the establishment of buprofezin immunoassay methods and provided valuable insights for the future modification of mAb-19F2 performance. Additionally, the study produced an ic-ELISA and GICA method based on mAb-19F2. The optimized ic-ELISA method had an  $IC_{50}$  value of 1.8  $\mu$ g/L, with a linear range of 0.6  $\mu$ g/L –5.4  $\mu$ g/L. On the other hand, the colloidal

gold test strip demonstrated an LOD of 500 ng/mL and an LOQ (IC<sub>20</sub>) of 16.8 µg/L. Both methods showed excellent recovery rates and no cross-reaction with neonicotinoid pesticides. Overall, this study offers essential biological raw materials for the immunoassay of buprofezin pesticide residues in food and agricultural products in China. Furthermore, it provides valuable guidance for the swift and accurate detection of buprofezin pesticide residues specifically in tea samples. The development of these new techniques and the novel insights gained into the recognition mechanism of haptens and mAb-19F2 can pave the way for the establishment of more reliable and sensitive buprofezin detection methods.

## Supplementary Material

Refer to Web version on PubMed Central for supplementary material.

## Acknowledgments

This study was financially supported by the National Natural Science Foundation of China (No. 32272423), NIEHS Superfund Research Program (No. P42 ES004699), Central Public Interest Scientific Institution Basal Research Fund for the Chinese Academy of Agricultural Sciences (No. Y2021PT05), and NIEHS RIVER AWARD (No. R35ES030443).

## References

- (1). Abdallah O; El Agamy M; Abdelraheem E; Malhat F Buprofezin Dissipation and Safety Assessment in Open Field Cabbage and Cauliflower Using GC/ITMS Employing an Analyte Protectant. *Biomedical Chromatography* 2019, 33 (6), e4492. 10.1002/bmc.4492. [PubMed: 30673143]
- (2). Wang Z; Zhou C; Long G; Yang H; Jin D Sublethal Effects of Buprofezin on Development, Reproduction, and Chitin Synthase 1 Gene (SfCHS1) Expression in the White-Backed Planthopper, *Sogatella furcifera* (Hemiptera: Delphacidae). *Journal of Asia-Pacific Entomology* 2018, 21 (2), 585–591. 10.1016/j.aspen.2018.03.009.
- (3). Control of insect pests with benzoylphenyl ureas | SpringerLink. [https://link.springer.com/chapter/10.1007/978-94-009-4824-2\\_9](https://link.springer.com/chapter/10.1007/978-94-009-4824-2_9) (accessed 2023-05-17).
- (4). Holmstrup M; Bindesbøl A-M; Oostingh GJ; Duschl A; Scheil V; Köhler H-R; Loureiro S; Soares AMVM; Ferreira ALG; Kienle C; Gerhardt A; Laskowski R; Kramarz PE; Bayley M; Svendsen C; Spurgeon DJ Interactions between Effects of Environmental Chemicals and Natural Stressors: A Review. *Science of The Total Environment* 2010, 408 (18), 3746–3762. 10.1016/j.scitotenv.2009.10.067. [PubMed: 19922980]
- (5). Sohail M; Khan SS; Muhammad R; Soomro QA; Asif MU; Solangi BK Impact of Insect Growth Regulators on Biology and Behavior of *Chrysoperla carnea* (Stephens) (Neuroptera: Chrysopidae). *Ecotoxicology* 2019, 28 (9), 1115–1125. 10.1007/s10646-019-02114-1. [PubMed: 31587131]
- (6). Liu T-X; Chen T-Y Effects of the Chitin Synthesis Inhibitor Buprofezin on Survival and Development of Immatures of *Chrysoperla rufilabris* (Neuroptera: Chrysopidae). *J Econ Entomol* 2000, 93 (2), 234–239. 10.1603/0022-0493-93.2.234. [PubMed: 10826167]
- (7). Ullah F; Gul H; Yousaf HK; Xiu W; Qian D; Gao X; Tariq K; Han P; Desneux N; Song D Impact of Low Lethal Concentrations of Buprofezin on Biological Traits and Expression Profile of Chitin Synthase 1 Gene (CHS1) in Melon Aphid, *Aphis gossypii*. *Sci Rep* 2019, 9 (1), 1–13. 10.1038/s41598-019-48199-w. [PubMed: 30626917]
- (8). Zeng B; Chen F; Liu Y; Guo D; Zhang Y; Feng Z; Wang L; Vontas J; Wu S; Zhu K; Gao C A chitin synthase mutation confers widespread resistance to buprofezin, a chitin synthesis inhibitor, in the brown planthopper, *Nilaparvata lugens*. *J. Pest sci.* 2023, 96, 819–823.

- (9). Su J; Wang Z; Zhang K; Tian X; Yin Y; Zhao X; Shen A; Gao CF Status of Insecticide Resistance of the Whitebacked Planthopper, *Sogatella Furcifera* (Hemiptera: Delphacidae). *The Florida Entomologist* 2013, 96 (3), 948–956.
- (10). Qureshi IZ; Bibi A; Shahid S; Ghazanfar M Exposure to Sub-Acute Doses of Fipronil and Buprofezin in Combination or Alone Induces Biochemical, Hematological, Histopathological and Genotoxic Damage in Common Carp (*Cyprinus Carpio* L.). *Aquatic Toxicology* 2016, 179, 103–114. 10.1016/j.aquatox.2016.08.012. [PubMed: 27595653]
- (11). Marimuthu K; Muthu N; Xavier R; Arockiaraj J; Rahman MA; Subramaniam S Toxicity of Buprofezin on the Survival of Embryo and Larvae of African Catfish, *Clarias Gariepinus* (Bloch). *PLoS ONE* 2013, 8 (10), e75545. 10.1371/journal.pone.0075545. [PubMed: 24098390]
- (12). Ku T; Yan W; Jia W; Yun Y; Zhu N; Li G; Sang N Characterization of Synergistic Embryotoxicity of Nickel and Buprofezin in Zebrafish. *Environ. Sci. Technol.* 2015, 49 (7), 4600–4608. 10.1021/es506293t. [PubMed: 25790023]
- (13). Ding Y; Hua X; Chen H; Gonzalez-Sapienza G; Barnych B; Liu F; Wang M; Hammock BD A Dual Signal Immunochromatographic Strip for the Detection of Imidaclothiz Using a Recombinant Fluorescent-Peptide Tracer and Gold Nanoparticles. *Sensors and Actuators B: Chemical.* 2019, 297, 126714. 10.1016/j.snb.2019.126714.
- (14). Gawel M; Kiljanek T; Niewiadowska A; Semeniuk S; Goliszek M; Burek O; Posyniak A Determination of Neonicotinoids and 199 Other Pesticide Residues in Honey by Liquid and Gas Chromatography Coupled with Tandem Mass Spectrometry. *Food Chemistry* 2019, 282, 36–47. 10.1016/j.foodchem.2019.01.003. [PubMed: 30711104]
- (15). Di Muccio A; Fidente P; Barbini DA; Dommarco R; Seccia S; Morrica P Application of Solid-Phase Extraction and Liquid Chromatography–Mass Spectrometry to the Determination of Neonicotinoid Pesticide Residues in Fruit and Vegetables. *Journal of Chromatography A* 2006, 1108 (1), 1–6. 10.1016/j.chroma.2005.12.111. [PubMed: 16448655]
- (16). Xu L; Abd El-Aty AM; Eun J-B; Shim J-H; Zhao J; Lei X; Gao S; She Y; Jin F; Wang J; Jin M; Hammock BD Recent Advances in Rapid Detection Techniques for Pesticide Residue: A Review. *J. Agric. Food Chem.* 2022, 70 (41), 13093–13117. 10.1021/acs.jafc.2c05284. [PubMed: 36210513]
- (17). Ding J; Mei S; Gao L; Wang Q; Ma H; Chen X Tea processing steps affect chemical compositions, enzyme activities, and antioxidant and anti-inflammatory activities of coffee leaves. *Food Frontiers.* 2022, 3, 505–516. 10.1002/fft2.136.
- (18). Your gateway to the EU, News, Highlights | European Union. [https://european-union.europa.eu/index\\_en](https://european-union.europa.eu/index_en) (accessed 2023-04-06).
- (19). Search engine for MRLs of Agricultural Chemicals in Foods. <http://db.ffcr.or.jp/front/> (accessed 2023-04-06).
- (20). Xu L; Abd El-Aty AM; Shim J-H; Eun J-B; Lei X; Zhao J; Zhang X; Cui X; She Y; Jin F; Zheng L; Wang J; Jin M; Hammock BD Design and Characterization of a Novel Hapten and Preparation of Monoclonal Antibody for Detecting Atrazine. *Foods* 2022, 11 (12), 1726. 10.3390/foods11121726. [PubMed: 35741925]
- (21). Xu L; Abd El-Aty AM; Zhao J; Lei X; Zhang X; Zhao Y; Cui X; She Y; Jin F; Wang J; Jin M; Hammock BD Obtaining a Monoclonal Antibody against a Novel Prometryn-Like Hapten and Characterization of Its Selectivity for Triazine Herbicides. *Biosensors* 2023, 13 (1), 22. 10.3390/bios13010022.
- (22). Goodrow MH; Harrison RO; Hammock BD Hapten Synthesis, Antibody Development, and Competitive Inhibition Enzyme Immunoassay for s-Triazine Herbicides. *J. Agric. Food Chem.* 1990, 38 (4), 990–996. 10.1021/jf00094a016.

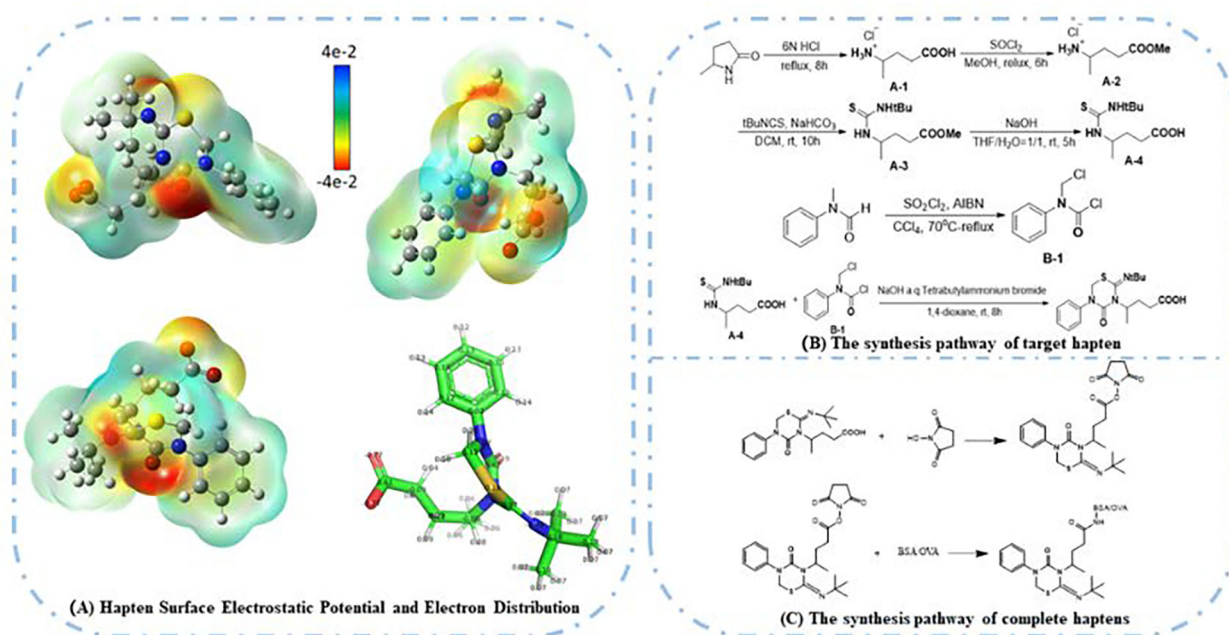


**Figure 1.** Design and synthesis of haptens as well as the synthesis of complete antigens.

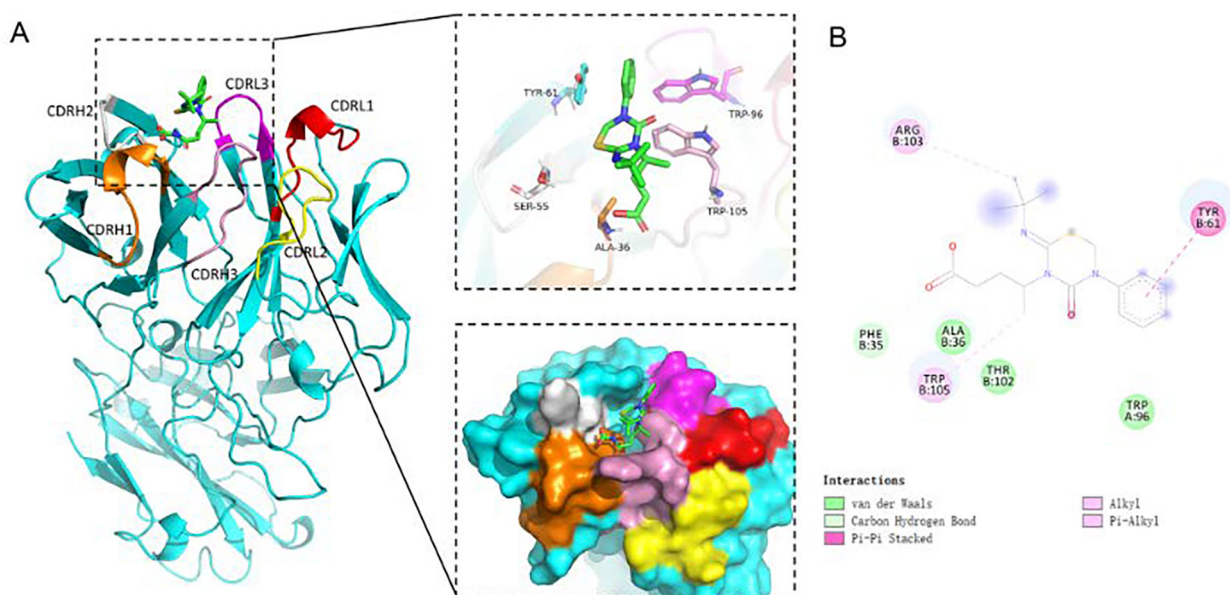


**Figure 2.** Binding mode of hapten to mAb-19F2 protein ((A) Overall view of small molecules and protein binding, partial 3D view. In the figure, green sticks represent small molecules, and different colors represent different loop regions. (B) 2D interaction diagram).

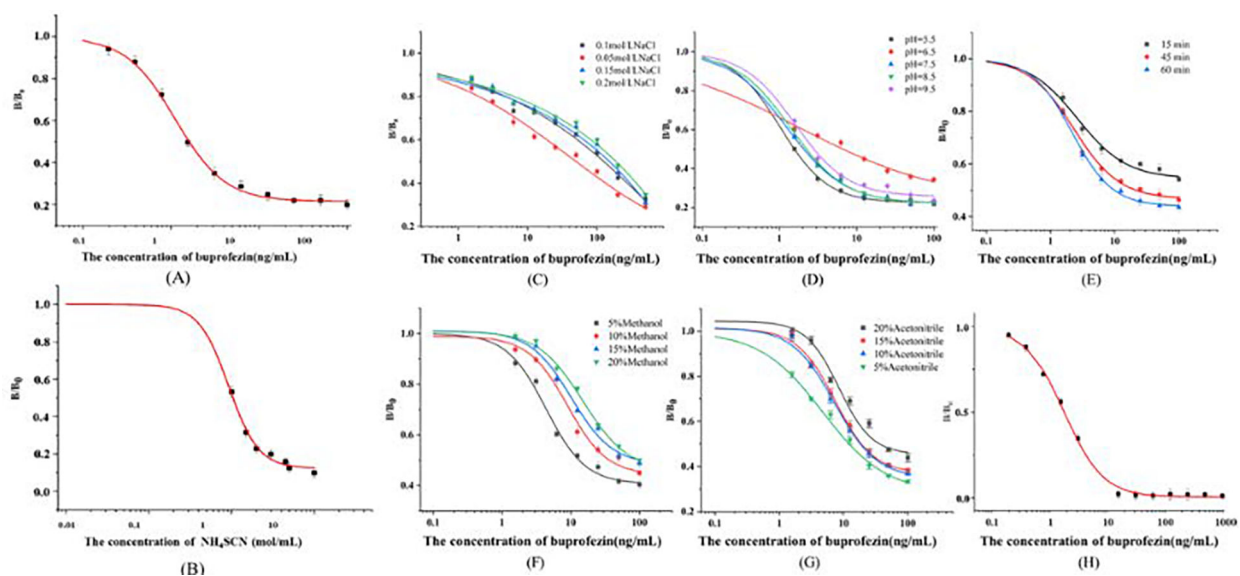


**Figure 3.** The results were determined using ic-ELISA: (A) the unoptimized conditions of mAb-19F2 were used to fit the standard curve, (B-G) the optimized conditions of ic-ELISA were used to measure the results, and (H) the optimized conditions of mAb-19F2 were used to fit the standard curve.

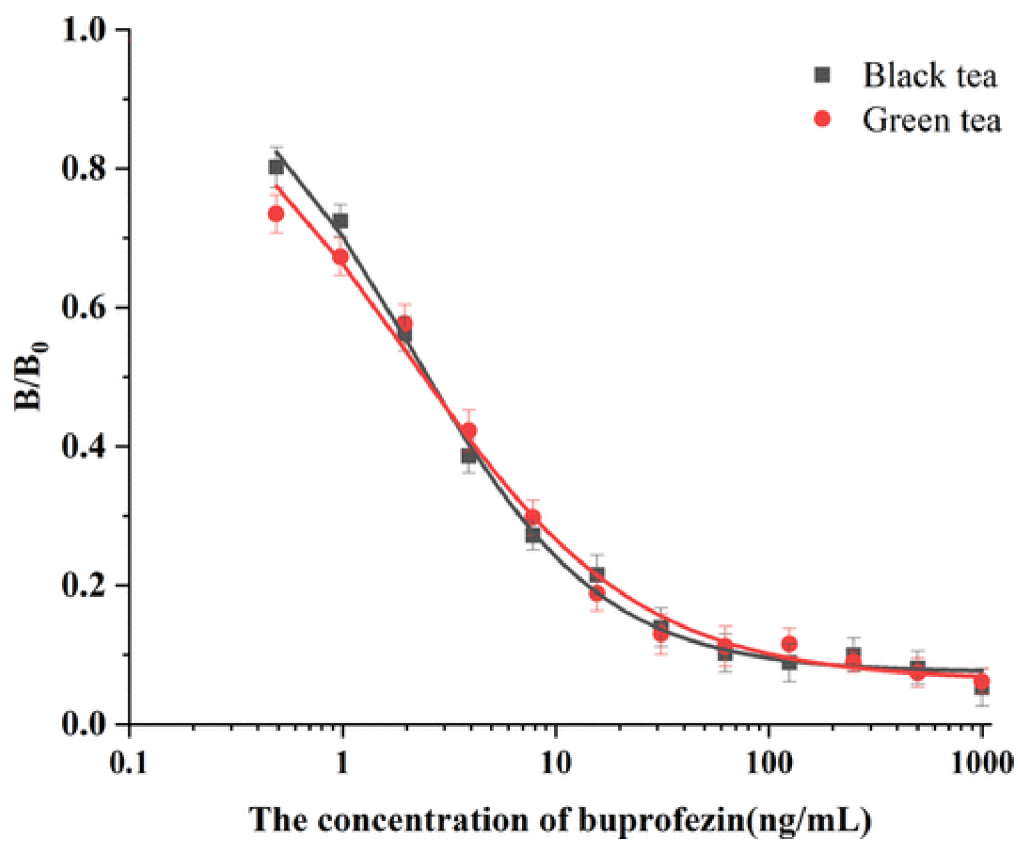


**Figure 4.**  
Matrix standard curves for black and green tea.

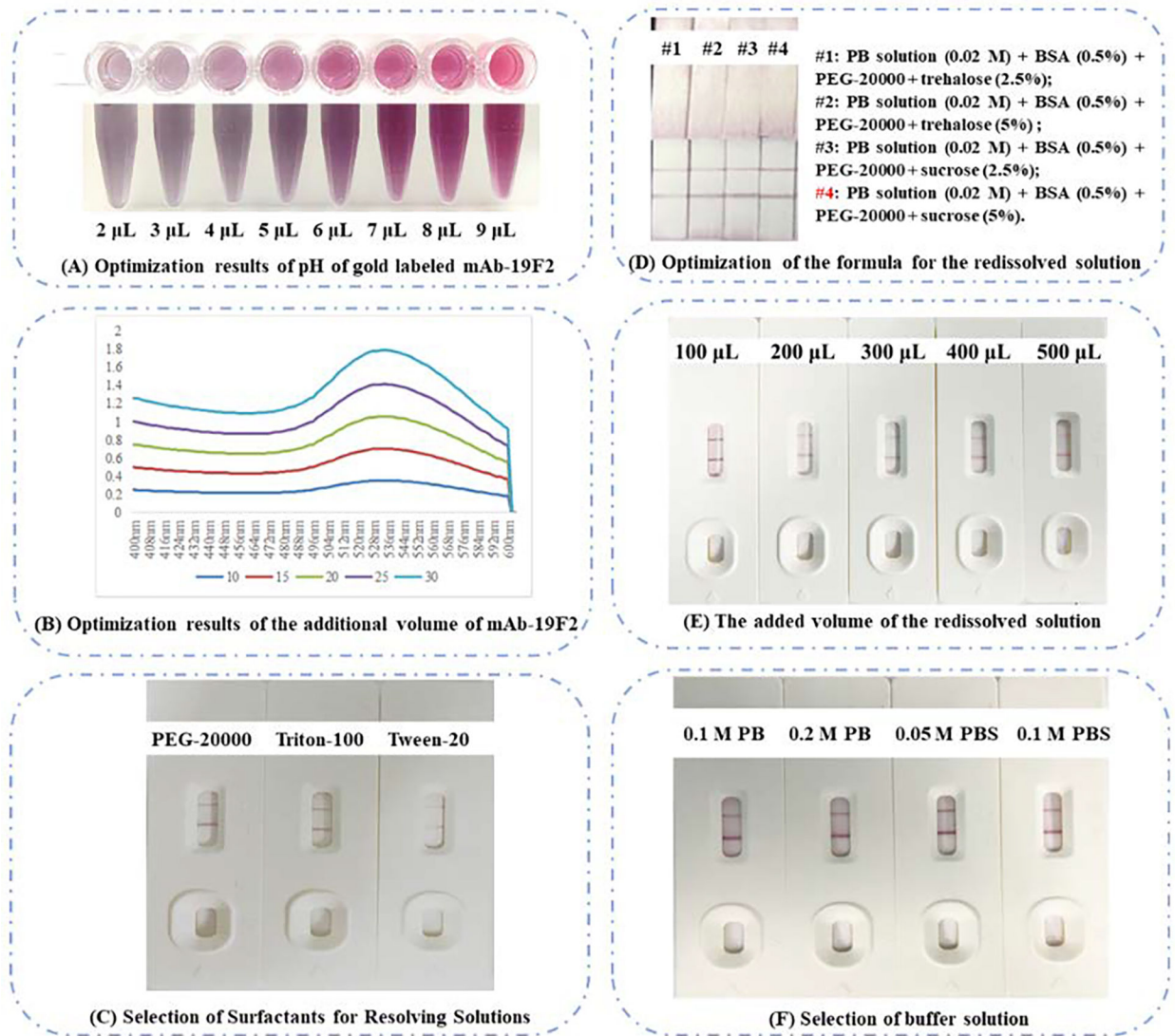


**Figure 5.**  
 Optimization results of conditions for GICA.



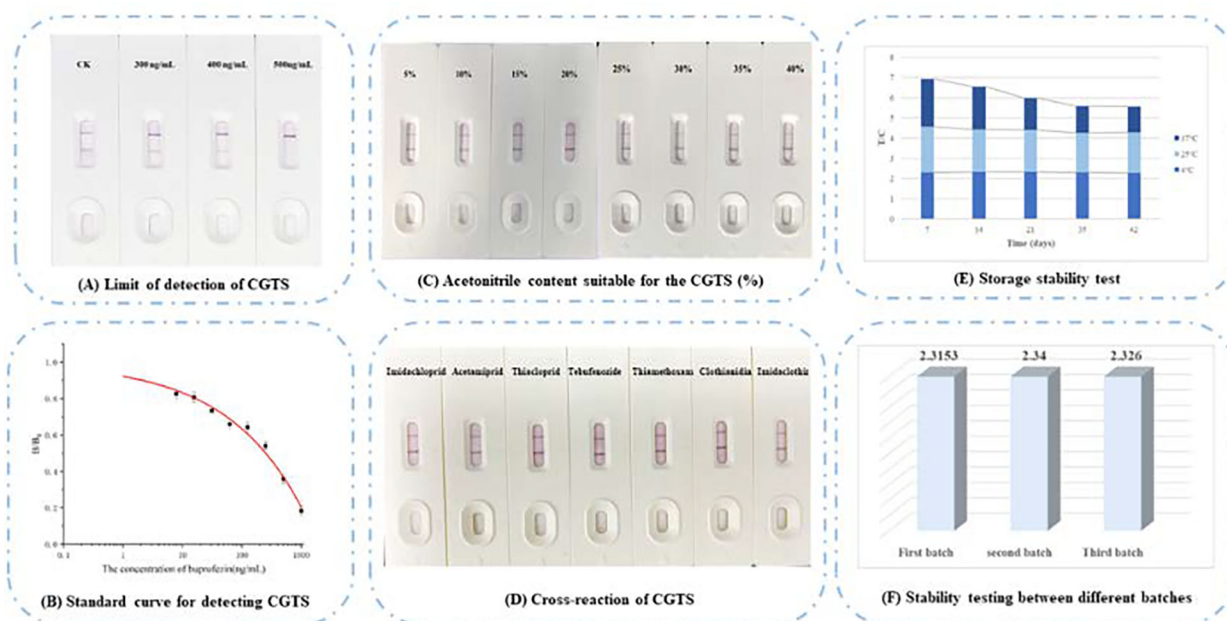


**Figure 6.**  
Performance evaluation results of GICA.

**Table 1.**

Immunoantigen synthesis results.

Immunoantigen				
Feed ratio	Molecular weight (Da)	$\Delta M$	Coupling ratio	Number of couplings
30:01:00	71313.012	3978.732	10.956	10
40:01:00	71444.249	4109.969	11.317	11
50:01:00	71829.991	4495.711	12.38	12
60:01:00	73251.55	5917.27	16.294	16
Coating antigen				
20:01	45380.114	1227.614	3.38	3
30:01:00	45718.097	1565.597	4.311	4
40:01:00	45842.67	1690.17	4.654	4
50:01:00	45925.071	1772.571	4.881	4

Author Manuscript

Author Manuscript

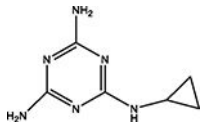
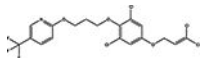
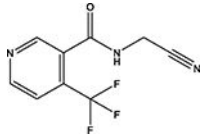
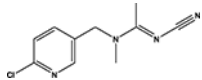
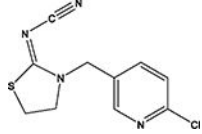
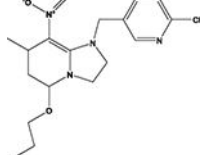
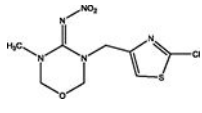
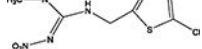
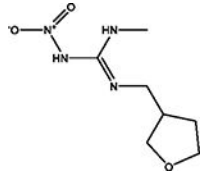
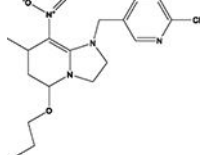
Author Manuscript

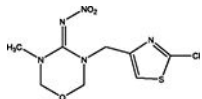
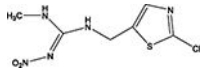
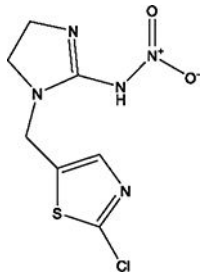
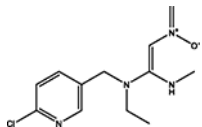
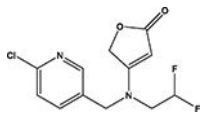
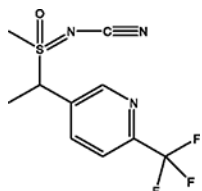
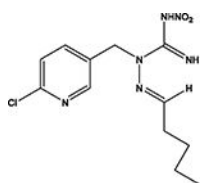
Author Manuscript

**Table 2.**

Cross reaction of mab-19F2 with other pesticides

Name	Chemical structural	IC <sub>50</sub> (ng/mL)	Cross-reactivity (%)
Buprofezin		1.81	100%
Tebufenozide		>1000	<0.18%
Lufenuron		>1000	<0.18%
Chlorfluazuron		>1000	<0.18%
Triflumuron		>1000	<0.18%
Diflubenzuron		>1000	<0.18%
Chlorbenzuron		>1000	<0.18%
Hexaflumuron		>1000	<0.18%
1,2-dibenzoyl-1-(t-butyl)hydrazine		>1000	<0.18%
Pyriproxyfen		>1000	<0.18%
Chromafenozide		>1000	<0.18%
Fenoxycarb		>1000	<0.18%

Name	Chemical structural	IC <sub>50</sub> (ng/mL)	Cross-reactivity (%)
Cyromazine		>1000	<0.18%
Pyridalyl		>1000	<0.18%
Flonicamid		>1000	<0.18%
Acetamiprid		>1000	<0.18%
(E)-Thiacloprid		>1000	<0.18%
Paichongding(IPP)		>1000	<0.18%
Thiamethoxam		>1000	<0.18%
Clothianidin		>1000	<0.18%
Dinotefuran		>1000	<0.18%
Paichongding		>1000	<0.18%

Name	Chemical structural	IC <sub>50</sub> (ng/mL)	Cross-reactivity (%)
Thiamethoxam		>1000	<0.18%
Clothianidin		>1000	<0.18%
Imidaclothiz		>1000	<0.18%
Nitenpyram		>1000	<0.18%
Flupyradifurone		>1000	<0.18%
Sulfoxaflor		>1000	<0.18%
Guadipyr		>1000	<0.18%

Note: The maximum inhibitory concentration of other pesticides was 1000 ng/mL.

**Table 3.**

Antibody type of mAb-19F2.

Antibody type	IgG <sub>2a</sub>	IgG <sub>2b</sub>	IgG <sub>3</sub>	IgM	IgA	IgG <sub>1</sub>
	0.4868	0.5406	0.5301	0.5934	0.4602	1.4212
OD <sub>450nm</sub>	0.4652	0.558	0.5254	0.5897	0.4315	1.4433
	0.4586	0.5462	0.5143	0.6019	0.4549	1.3863

Author Manuscript

Author Manuscript

Author Manuscript

Author Manuscript

**Table 4.**

The optimal dilution concentration combination.

<b>Optimal dilution combination for C-line and T-line</b>				
T-line concentration (mg/mL)	1	0.8	0.5	0.3
Blank T/C value	1.68	1.24	1.1	0.97
C-line concentration (mg/mL)	2	1.5	1	0.5
Blank T/C value	1.38	2.26	3.98	4.34

Author Manuscript

Author Manuscript

Author Manuscript

Author Manuscript

**Table 5.**

Determination of the recovery rate in Tea using LC/MS.

Varieties of tea	Spiked concentration	LC-MS			Ic-ELISA			GICT		
	(mg/kg)	Measured concentration (mg/kg)	Recovery (%)	RSD (%)	Measured concentration (mg/kg)	Recovery (%)	RSD (%)	Measured concentration (mg/kg)	Recovery (%)	RSD (%)
Black tea	2.5	2.32±0.18	92.85±7.00	7.5	2.51±0.81	100.26±3.25	3.2	2.12±0.11	84.8±4.40	4.2
	5	5.27±1.02	117.15±3.18	2.7	5.04±0.20	100.96±3.92	3.8	4.61±0.32	92.2±6.34	6.6
	10	9.285±0.70	92.85±7.00	7.5	4.80±0.10	96.00±1.98	2.1	8.95±0.61	89.5±6.06	6.3
Green tea	2.5	2.76±0.21	110.33±8.59	7.8	2.43±0.09	97.13±3.75	3.8	2.09±0.21	83.6±8.40	8.6
	5	5.27±0.16	105.35±3.18	3	4.63±0.23	92.40±4.53	4.8	4.58±0.47	91.6±9.45	9.9
	10	11.31±0.77	113.1±7.75	6.8	9.70±0.44	97.04±4.36	4.5	8.49±0.71	84.9±7.12	7.5